

Method to Control Dynamic Snap-Through Instability of Dielectric Elastomers

Junshi Zhang,^{1,2} Hualing Chen,^{1,3,*} and Dichen Li^{1,2}

¹*School of Mechanical Engineering, Xi'an Jiaotong University, Xi'an 710049, China*

²*State Key Laboratory for Manufacturing Systems Engineering, Xi'an Jiaotong University, Xi'an 710054, China*

³*State Key Laboratory for Strength and Vibration of Mechanical Structures, Xi'an Jiaotong University, Xi'an 710049, China*

(Received 26 July 2016; revised manuscript received 9 November 2016; published 23 December 2016)

Dielectric elastomers (DEs) are a category of soft materials that are capable of large deformation, however, the actuation performance is affected by snap-through instability. In this article, a dynamics model is developed to investigate the dynamic snap-through instability of DEs by applying the triangle and sinusoidal voltages. The DE materials with different limiting stretches are considered. When the DE is under a triangle voltage or a sinusoidal voltage, the snap-through behavior may emerge during the response in time domain, and the DEs with a large value of limiting stretch are susceptible to dynamic snap-through instability. By tuning the mechanical tensile force, the occurrence of dynamic snap-through instability can be controlled. With the increase of tensile force, the dynamic snap-through behavior initially does not emerge during vibration, then accompanies the vibration, and eventually disappears. Phase paths and Poincaré maps are utilized to explore the dynamic stability evolution of the DE systems.

DOI: [10.1103/PhysRevApplied.6.064012](https://doi.org/10.1103/PhysRevApplied.6.064012)

I. INTRODUCTION

Dielectric elastomers (DEs) are a category of soft membranes that can shrink in thickness and expand in area [1–5]. The induced strains can be up to 100% [1]. Therefore, DEs are generally considered for biological materials and artificial muscles [3]. Recently, DEs have gained sustaining and significant investigation in the electromechanical field, and they are applied in a wide range of applications, such as spring-roll actuators [6,7], tunable lenses [8,9], loudspeakers [10], acoustic actuators [11], and energy generators [12,13].

In view of their versatile properties, DEs are admirable candidates for musclelike soft actuators. However, DEs are susceptible to emerging electromechanical instabilities (EMI) during the actuation process [4,14–17]. Typical EMI phenomena include pull-in instability [18] and snap-through instability [4]. When a DE membrane is subject to a high voltage, the induced Maxwell stress squeezes the membrane, causing a further-enhanced electrical field. The electrical field will further compress the DE membrane. This positive feedback may generate the pull-in instability of DEs, which plays an essential role in hindering the large stable actuation of DEs.

After the pull-in instability, the elastomer can survive without electrical breakdown; instead, it may be stabilized in a state of a much smaller thickness, resulting in a snap-through instability [4]. When the elastomer is actuated by

voltage, the voltage-stretch curve may take an N-shaped form [4,14,15], that is, snap-through behavior happens. Snap-through instability is likely to induce the electrical breakdown and tearing failure of the DE membrane. To overcome this unwelcome issue, some attempts have been performed, and the corresponding methods are proposed, such as prestretch [15,19], the pure-shear deformation mode [19,20], and charge-controlled actuation [21,22]. These strategies can certainly suppress the snap-through behavior in DE actuation. Unfortunately, almost all the reported work related to snap-through instability focuses on static deformation, without involving dynamic snap-through instability. However, to perform as electromechanical actuators, e.g., frequency tuning [23], pumps [24], and acoustic actuators [11], DEs are mostly expected to operate under the alternating load. Recently, by employing a structure of the DE balloon and incorporating pneumatic pressure, Chen *et al.* [25] studied four types of oscillation and analyzed the results, taking account of the dynamic snap-through instability. However, a method to overcome and control this undesirable dynamic snap-through instability is still not investigated, which is definitely worth being explored.

Admittedly, most workhorse DE materials belong to a class of macromolecular polymers, such as polyacrylate [26], polydimethylsiloxane [27], silicone [28], and rubber [29]. The dissipative characteristics, such as viscoelasticity, will certainly affect the actuation process, especially for the VHB-based elastomer [26]. However, in this paper, the performance and overcoming method of dynamic snap-through instability of DEs are the main focuses. In order to

*Corresponding author.
hlchen@mail.xjtu.edu.cn

simplify the modeling work, we adopt the ideally hyperelastic DEs [30,31] and neglect the effect of viscoelasticity.

To investigate the dynamic performance, the triangle and sinusoidal voltages are applied to actuate the DEs, respectively. Dynamic snap-through instability under the stimulation of these two waveform voltages is studied. The results indicate that the snap-through behavior perhaps emerges during the response in time domain, which is also determined by the value of the limiting stretch of the DE material. In the following, the method to control the dynamic snap-through instability is explored by utilizing a mechanical force. With the increase of tensile force, the dynamic snap-through behavior initially does not emerge, then accompanies the vibration, and disappears eventually. We also analyze the stability evolution of vibration under different actuated voltage and mechanical forces through the phase paths and Poincaré maps.

II. DYNAMICS MODEL OF THE DE SYSTEM

A square DE membrane of initial length L and thickness H in the reference state is employed to develop the dynamics model, as shown in Fig. 1(a). The DE membrane is coated with compliant electrodes on both surfaces. Subject to an equibiaxial and homogenous tensile force P , and a voltage ϕ through the thickness direction, the DE deforms to length l , and thickness h , as shown in Fig. 1(b). We define the stretch in the in-plane direction as $\lambda = l/L$. By assuming the incompressibility of DEs [31], we obtain the stretch in the thickness direction as $\lambda_h = h/H = \lambda^{-2}$. When an ac voltage is applied, the DE membrane vibrates. To analyze the dynamic electromechanical behavior, the inertial forces should be included when deriving the governing equations. During the process of actuation, the total work done by the inertial force is calculated by integrating along the three principle directions [32]; whereas, the inertial force in the thickness direction is neglected, as the size of the thickness is much smaller than that in the in-plane direction [33]. As reported previously, the work done by the inertial force in the in-plane direction is obtained as $(-\rho L^4 H/3)(d^2\lambda/dt^2)\delta\lambda$ [32,34], where t denotes the time, and ρ is the density of the DE.

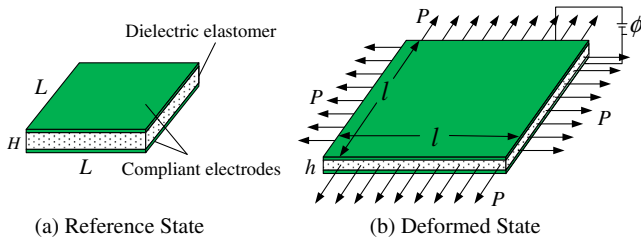


FIG. 1. (a) In the reference state, a DE membrane is of length L and thickness H . (b) In the deformed state, subject to the homogenous tensile force P and a voltage ϕ , the DE membrane has length l , and thickness h .

Suppose that the charge accumulated on the DE surfaces is Q , then the electrical displacement is obtained as $D = Q/(L^2\lambda^2)$. The thermodynamics of an ideal DE is characterized by the density of the Helmholtz free energy $W(\lambda, D)$. To account for the behavior of strain stiffening, the Gent model [35] is adopted in this article. Therefore, based on the assumption of DE incompressibility, the free-energy density function is expressed as

$$W(\lambda, D) = -\frac{\mu J_{\text{lim}}}{2} \log\left(1 - \frac{2\lambda^2 + \lambda^{-4} - 3}{J_{\text{lim}}}\right) + \frac{D^2}{2\varepsilon}, \quad (1)$$

where ε is the permittivity, μ is the shear modulus, and J_{lim} is the material constant related to the limiting stretch, respectively.

In this paper, the ideal DEs are utilized, that is, the inherent viscoelasticity is ignored. Therefore, by employing the law of thermodynamics, we conclude that variation of the free energy of the DE is equal to the work done jointly by the voltage, the tensile force, and the inertial force

$$L^2 H \delta W = \phi \delta Q + 2PL\delta\lambda - \frac{2\rho L^4 H}{3} \frac{d^2\lambda}{dt^2} \delta\lambda. \quad (2)$$

The variation of charge Q can be expressed as

$$\delta Q = L^2 \lambda^2 \delta D + 2DL^2 \lambda \delta\lambda. \quad (3)$$

Combining Eqs. (1)–(3), the governing equation of the dynamical DE system can be yielded as

$$\frac{\rho L^2}{3\mu} \frac{d^2\lambda}{dt^2} + \frac{\lambda - \lambda^{-5}}{1 - (2\lambda^2 + \lambda^{-4} - 3)/J_{\text{lim}}} - \frac{P}{\mu LH} - \frac{\varepsilon\phi^2}{\mu H^2} \lambda^3 = 0. \quad (4)$$

To be more general, the variables are simplified to be nondimensionalized. Consequently, Eq. (4) can be reexpressed in the following form:

$$\frac{d^2\lambda}{dT^2} + \frac{\lambda - \lambda^{-5}}{1 - (2\lambda^2 + \lambda^{-4} - 3)/J_{\text{lim}}} - \frac{P}{\mu LH} - \frac{\varepsilon\phi^2}{\mu H^2} \lambda^3 = 0, \quad (5)$$

where $T = t/\sqrt{\rho L^2/3\mu}$ is the dimensionless time, $P/(\mu LH)$ is the dimensionless mechanical force, and $\phi/(H\sqrt{\mu/\varepsilon})$ is the dimensionless voltage.

III. STATIC SNAP-THROUGH INSTABILITY

First, we reexplore the snap-through behavior of DE under dc voltage by taking into account different values of J_{lim} [30]. Under such a condition, the inertial force is neglected [15,19,20]. Thus, Eq. (5) reduces to

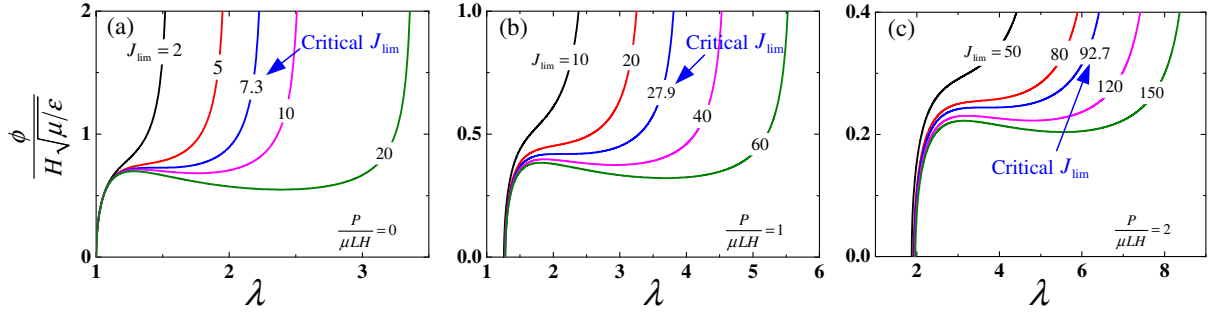


FIG. 2. The voltage-stretch curves of DE under different values of tensile force P . (a) $P/(\mu LH) = 0$, (b) $P/(\mu LH) = 1$, (c) $P/(\mu LH) = 2$. With increasing the value of J_{lim} , the actuation of DE evolves from stability to snap-through instability.

$$\frac{\phi}{H\sqrt{\mu/\varepsilon}} = \sqrt{\frac{\lambda^{-2} - \lambda^{-8}}{1 - (2\lambda^2 + \lambda^{-4} - 3)/J_{\text{lim}}} - \frac{P}{\mu LH}} \lambda^{-3}. \quad (6)$$

Figure 2 illustrates the voltage-stretch curves of DE under different values of dimensionless tensile force. Under a constant tensile force, the voltage-stretch curve of DE evolves from monotonically increasing to N shaped with the enlargement of J_{lim} , that is, the actuation property of DE changes from stable to unstable with increasing J_{lim} . As indicated in Fig. 2, the critical J_{lim} of transition from stable to unstable is 7.3 [$P/(\mu LH) = 0$], 27.9 [$P/(\mu LH) = 1$], and 92.7 [$P/(\mu LH) = 2$], respectively. This suggests that mechanical force adds the critical J_{lim} and enhances the actuation stability, which is consistent with other reported works [14,15,19]. The critical J_{lim} can be obtained by calculating the first-order derivative of dimensionless voltage versus stretch, that is, $d\phi/(H\sqrt{\mu/\varepsilon}d\lambda)$. If the value of J_{lim} satisfies the condition that only one zero point of $d\phi/(H\sqrt{\mu/\varepsilon}d\lambda)$ exists, then this J_{lim} is the critical

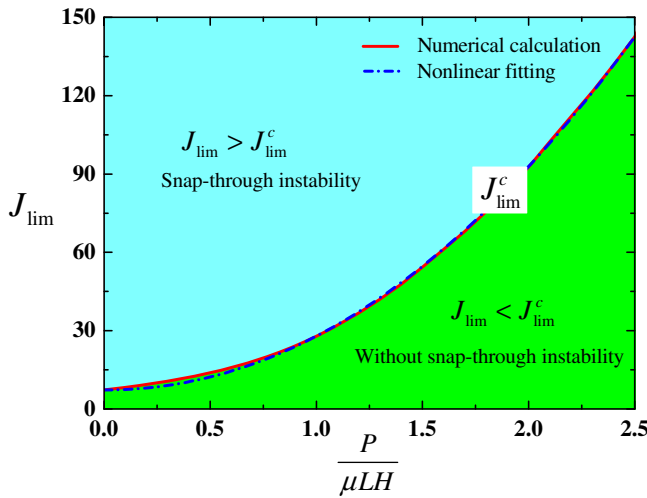


FIG. 3. Relationship between the critical J_{lim} of DE, J_{lim}^c , and dimensionless tensile force. When $J_{\text{lim}} > J_{\text{lim}}^c$, the snap-through emerges, while $J_{\text{lim}} < J_{\text{lim}}^c$, the snap-through does not emerge.

one. In the following, we define the critical J_{lim} of stability transition as J_{lim}^c .

Furthermore, the continuous relationship between J_{lim}^c and $P/(\mu LH)$ is plotted by the red solid curve in Fig. 3. Since J_{lim}^c is calculated numerically, a nonlinear fitting is applied by assuming an analytic exponential formula. The fitting result is obtained as $J_{\text{lim}}^c = 20.6[P/(\mu LH)]^{2.05} + 7.31$, as shown by the blue dashed curve in Fig. 3. With the increase of $P/(\mu LH)$, J_{lim}^c initially enlarges slowly, and subsequently enlarges dramatically. Under each value of $P/(\mu LH)$, when $J_{\text{lim}} > J_{\text{lim}}^c$, the snap-through behavior emerges, while $J_{\text{lim}} < J_{\text{lim}}^c$, the snap-through behavior does not emerge. This result can help to guide the practical applications to avoid the snap-through instability by selecting the required DE materials of suitable J_{lim} with incorporation of the different mechanical tensile forces.

IV. ANALYSES ABOUT DYNAMIC SNAP-THROUGH INSTABILITY

In this section, we carry out the analyses about dynamic snap-through instability by applying the triangle and sinusoidal voltages. Figure 4 sketches the snap-through behavior of DEs [14,36]. When the applied voltage increases, the stretch enlarges continuously from point O

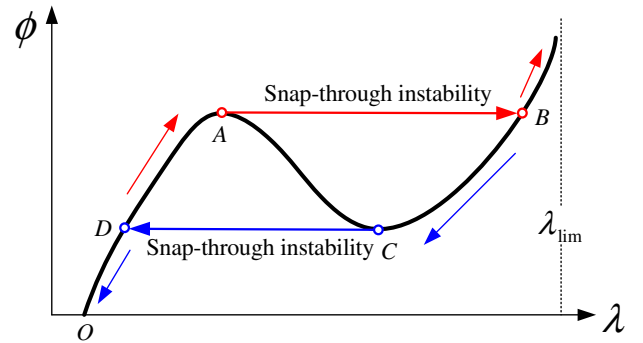


FIG. 4. Schematic of the snap-through behavior. When the voltage adds to point A , the stretch snaps from A to B , and then enlarges gradually; when the voltage drops to point C , the stretch snaps from C to D , and then reduces gradually.

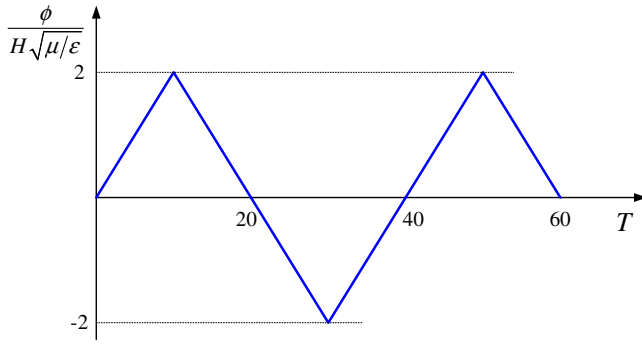


FIG. 5. A cycled triangle voltage with a dimensionless maximum voltage of $\phi/(H\sqrt{\mu/\epsilon}) = \pm 2$ and a dimensionless period of $T = 40$.

to point A. After point A, the stretch continues to increase, while the voltage drops down. However, in practical actuation, the applied voltage is kept increased, resulting in a snap-through behavior from point A to point B. On the other hand, when the voltage decreases, the stretch first reduces gradually from point B to point C. After point C, the stretch continues to decrease, while the required voltage should be enlarged. In practical actuation, the applied voltage is kept reducing, leading to the snap-through of the stretch from point C to point D.

A. Dynamic snap-through instability under a triangle voltage

In this subsection, we investigate the dynamic snap-through behavior of DEs under a cycled triangle voltage shown in Fig. 5. The maximum value of the dimensionless voltage is $\phi/(H\sqrt{\mu/\epsilon}) = \pm 2$, and the dimensionless period is $T = 40$. The dimensionless mechanical tensile force is prescribed as $P/(\mu LH) = 0$. As we know, the triangle voltage varies linearly, and the induced Maxwell stress generates the inertial force [37], which is included in our modeling.

Figure 6 describes the dynamic response of the DE by applying the cycled triangle voltage shown in Fig. 5. Under the circumstance of $J_{\text{lim}} = 2$, the stretch vibrates

continuously and gently in the time domain, as exhibited in Fig. 6(a). Figure 6(b) reveals the response of the DE with $J_{\text{lim}} = 20$. It is shown that the stretch initially vibrates continuously and strongly, and then suddenly the jumping behavior emerges.

When actuated by a triangle voltage, the DE may vibrate with snap-through behavior. Under the identical actuation, a DE with a larger value of J_{lim} will be susceptible to the dynamic snap-through instability. Therefore, the strategy that selects a DE material with a relatively small value of J_{lim} can avoid the dynamic snap-through instability during vibration.

B. Dynamic snap-through instability under a sinusoidal voltage

If the DE is stimulated by sinusoidal voltage, the deformation will be quite complicated. In this subsection, we define the applied sinusoidal voltage as

$$\phi = \phi_0 \sin(\omega t). \quad (7)$$

By utilizing the dimensionless time, Eq. (7) can be rewritten as $\phi = \phi_0 \sin(\Omega T)$, in which $\Omega = \omega \sqrt{\rho L^2/3\mu}$. Thus, Eq. (5) becomes

$$\frac{d^2 \lambda}{dT^2} + \frac{\lambda - \lambda^{-5}}{1 - (2\lambda^2 + \lambda^{-4} - 3)/J_{\text{lim}}} - \frac{P}{\mu LH} - \frac{\epsilon \phi_0^2}{\mu H^2} \lambda^3 \sin^2(\Omega T) = 0. \quad (8)$$

In the following calculation, we define $\Phi_0 = \phi_0/(H\sqrt{\mu/\epsilon})$ as the dimensionless amplitude of the applied sinusoidal voltage. In order to make a comparison with the actuation under triangle voltage, the dimensionless period of the sinusoidal voltage is assumed to be equal to the triangle voltage, namely, $T = 40$. Likewise, the dimensionless mechanical tensile force is also prescribed as $P/(\mu LH) = 0$.

Subject to the sinusoidal voltage, Fig. 7 plots the dynamic responses, phase paths, and Poincaré maps of

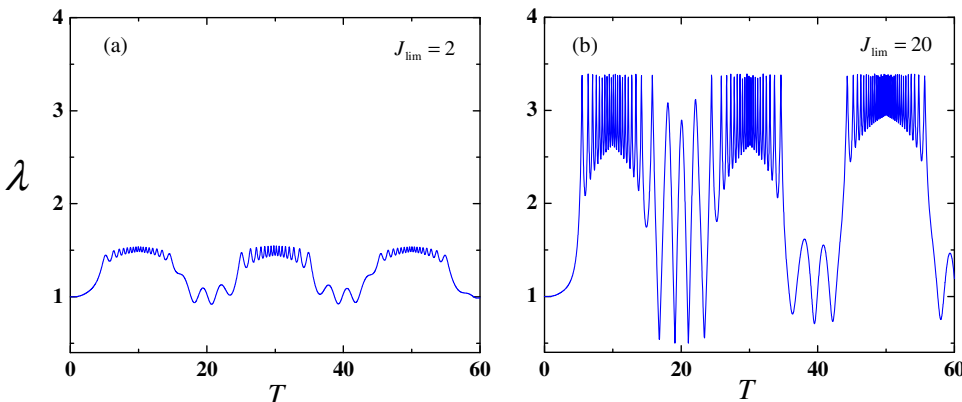


FIG. 6. Under the cycled triangle voltage in Fig. 5 and without tensile force, (a) the dynamic response of DE with the limiting stretch of $J_{\text{lim}} = 2$, and (b) the dynamic response of DE with the limiting stretch of $J_{\text{lim}} = 20$.

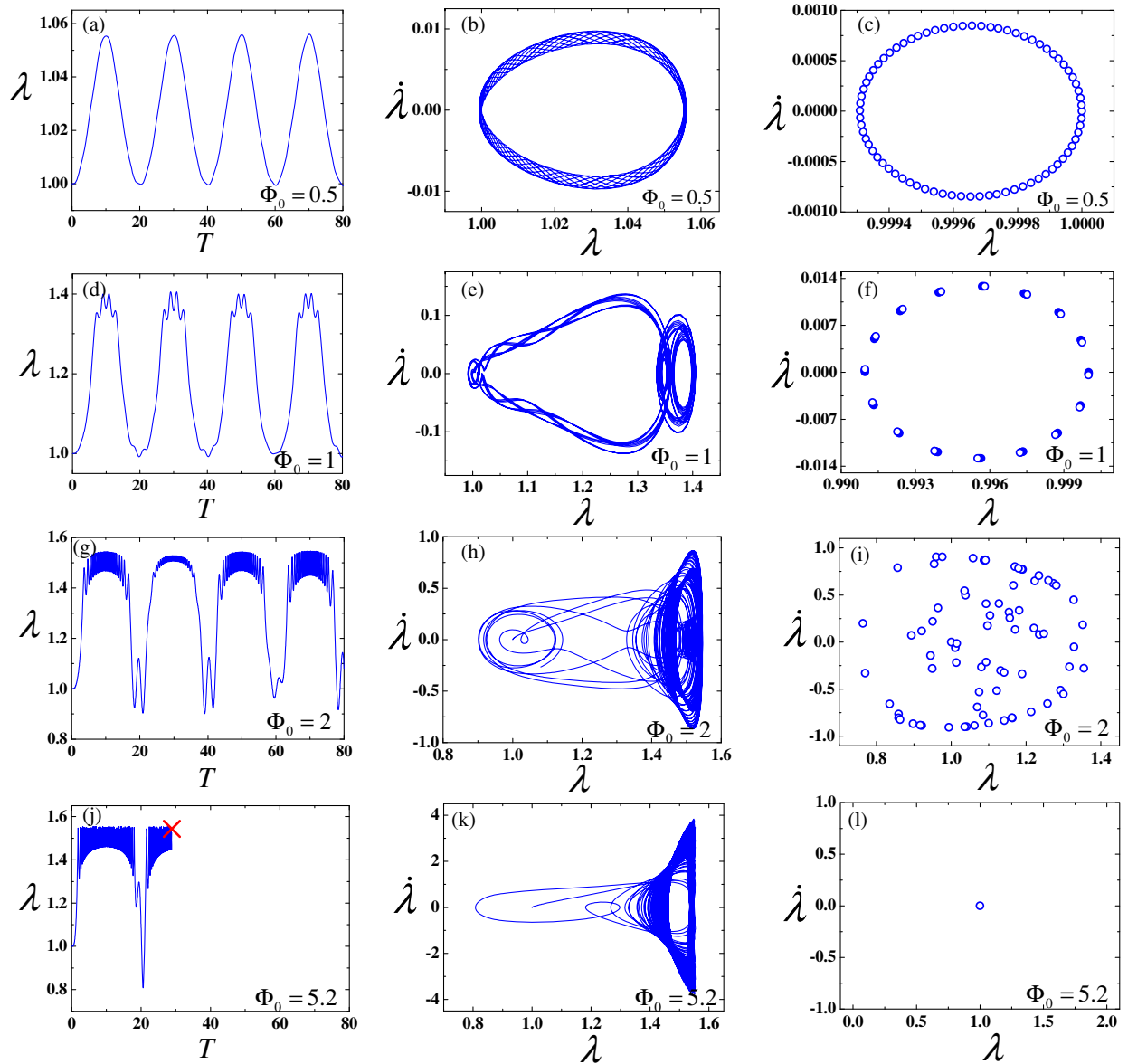


FIG. 7. Under sinusoidal voltage, the dynamic responses (a), (d), (g), (j); phase paths (b), (e), (h), (k); and Poincaré maps (c), (f), (i), (l) of DE with the limiting stretch of $J_{\text{lim}} = 2$. Four different dimensionless amplitudes of sinusoidal voltage are used in the calculation: $\Phi_0 = 0.5$ for (a), (b), (c); $\Phi_0 = 1$ for (d), (e), (f); $\Phi_0 = 2$ for (g), (h), (i); $\Phi_0 = 5.2$ for (j), (k), (l).

DE with the limiting stretch of $J_{\text{lim}} = 2$ by differing the dimensionless amplitude of the applied voltage. The phase paths and Poincaré maps are used to further detect the properties of dynamic DE systems. If all the points in Poincaré maps overlap to one point, the DE system experiences a periodic vibration. Meanwhile, if the points in Poincaré maps can form a closed loop, the DE system then undergoes a quasiperiodic vibration. On the contrary, if the points in Poincaré maps are disordered, the dynamic system experiences an aperiodic vibration. In the phase paths and Poincaré maps, λ means the first-order derivation of λ versus the dimensionless time, i.e., $\lambda = d\lambda/dT$. When Φ_0 is relatively smaller, such as $\Phi_0 = 0.5$ and $\Phi_0 = 1$, the

stretch vibrates stably and the dynamic snap-through behavior does not emerge in the response [Figs. 7(a) and 7(d)]. Also, the phase paths under $\Phi_0 = 0.5$ and $\Phi_0 = 1$ are presented in Figs. 7(b) and 7(e), indicative of a convergent closed loop. The related Poincaré maps [Figs. 7(c) and 7(f)] are ordered and form closed loops, demonstrating that the DE under $\Phi_0 = 0.5$ and $\Phi_0 = 1$ experiences a quasiperiodic vibration. However, with the increase of Φ_0 , take $\Phi_0 = 2$ as an example, the snap-through phenomenon emerges in the dynamic response of the stretch [Fig. 7(g)]. The stretch initially snaps to a large level and vibrates for a lasting period, and then snaps to a small value. The vibration almost centers around the large level, which is consistent to the dynamic response of DE under triangle voltage in

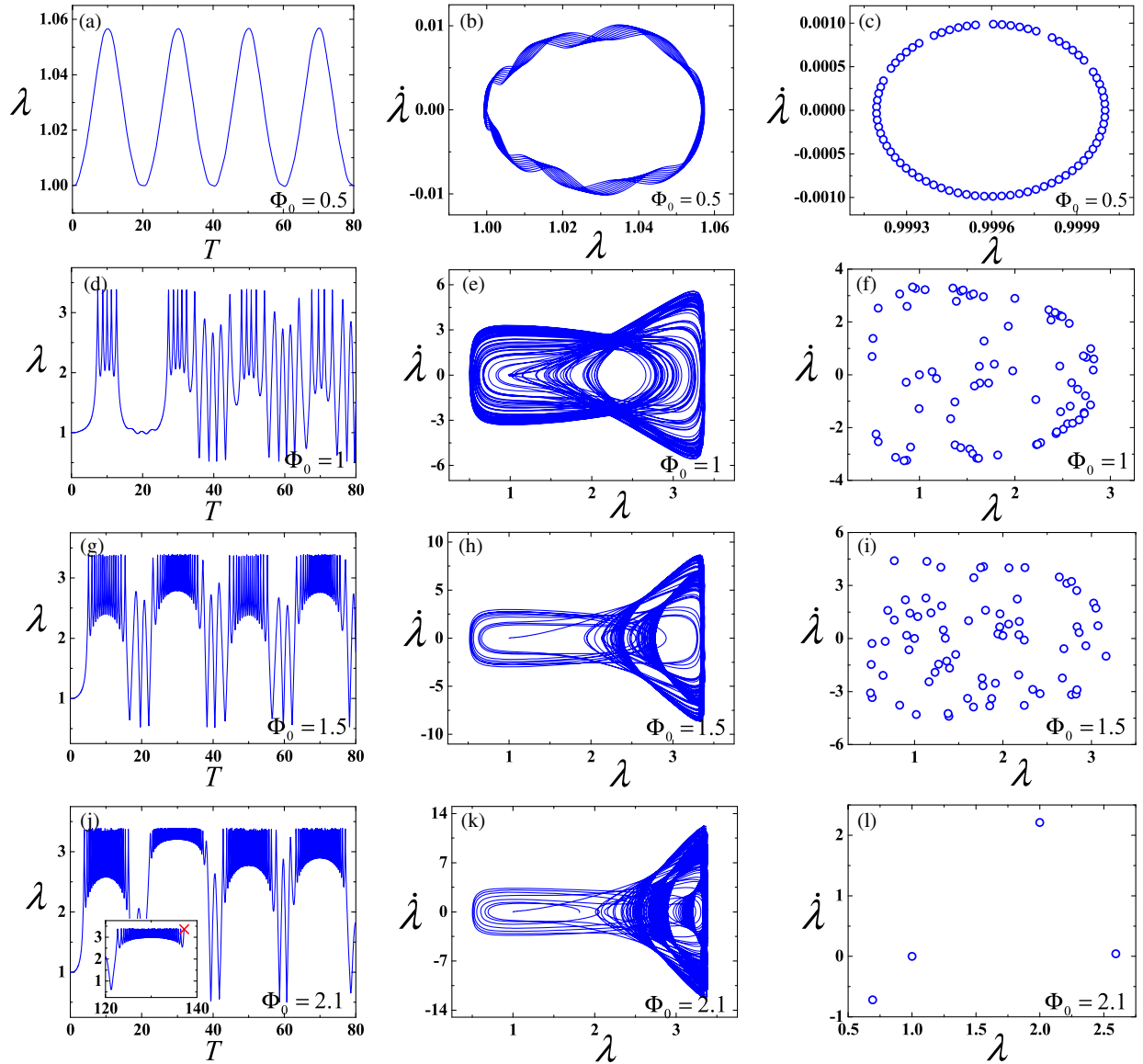


FIG. 8. Under sinusoidal voltage, the dynamic responses (a), (d), (g), (j); phase paths (b), (e), (h), (k); and Poincaré maps (c), (f), (i), (l) of DE with the limiting stretch of $J_{\text{lim}} = 20$. Four different dimensionless amplitudes of sinusoidal voltage are used in the calculation: $\Phi_0 = 0.5$ for (a), (b), (c); $\Phi_0 = 1$ for (d), (e), (f); $\Phi_0 = 1.5$ for (g), (h), (i); $\Phi_0 = 2.1$ for (j), (k), (l).

Fig. 6. The corresponding phase path in Fig. 7(h) also describes such a behavior. The Poincaré map under $\Phi_0 = 2$ is disordered and does not form a closed loop, indicating an aperiodic vibration, as illustrated in Fig. 7(i). If Φ_0 is further enlarged to a critical level, such as $\Phi_0 = 5.2$, the electromechanical failure behavior occurs in the dynamic actuation, Fig. 7(j). The phase path and Poincaré map under such a critical Φ_0 are provided in Figs. 7(k) and 7(l). It can be found that when the dynamic snap-through behavior occurs, the Poincaré maps show a disordered state, implying an aperiodic vibration; however, when the dynamic snap-through behavior is suppressed, the Poincaré maps transform to a closed loop, implying a quasiperiodic vibration. Dynamic snap-through instability strengthens

the nonlinearity of vibration. The reason that the vibrations become aperiodic may result from the strong nonlinearity induced by dynamic snap-through behaviors.

Similar to Fig. 7, Fig. 8 describes the dynamic responses, phase paths, and Poincaré maps of DE with the limiting stretch of $J_{\text{lim}} = 20$ by differing the dimensionless amplitude of the applied sinusoidal voltage. Similar results are concluded. When Φ_0 is small, the snap-through behavior does not emerge in the dynamic response, and the DE undergoes a quasiperiodic vibration, as sketched in Figs. 8(a)–8(c). With the increase of Φ_0 , the snap-through instability tends to appear during vibration, and the stability of the vibration evolves to be aperiodic, as plotted in Figs. 8(d)–8(i). Likewise, if Φ_0 is further enlarged to a critical level, such as $\Phi_0 = 2.1$, the electromechanical failure behavior occurs in

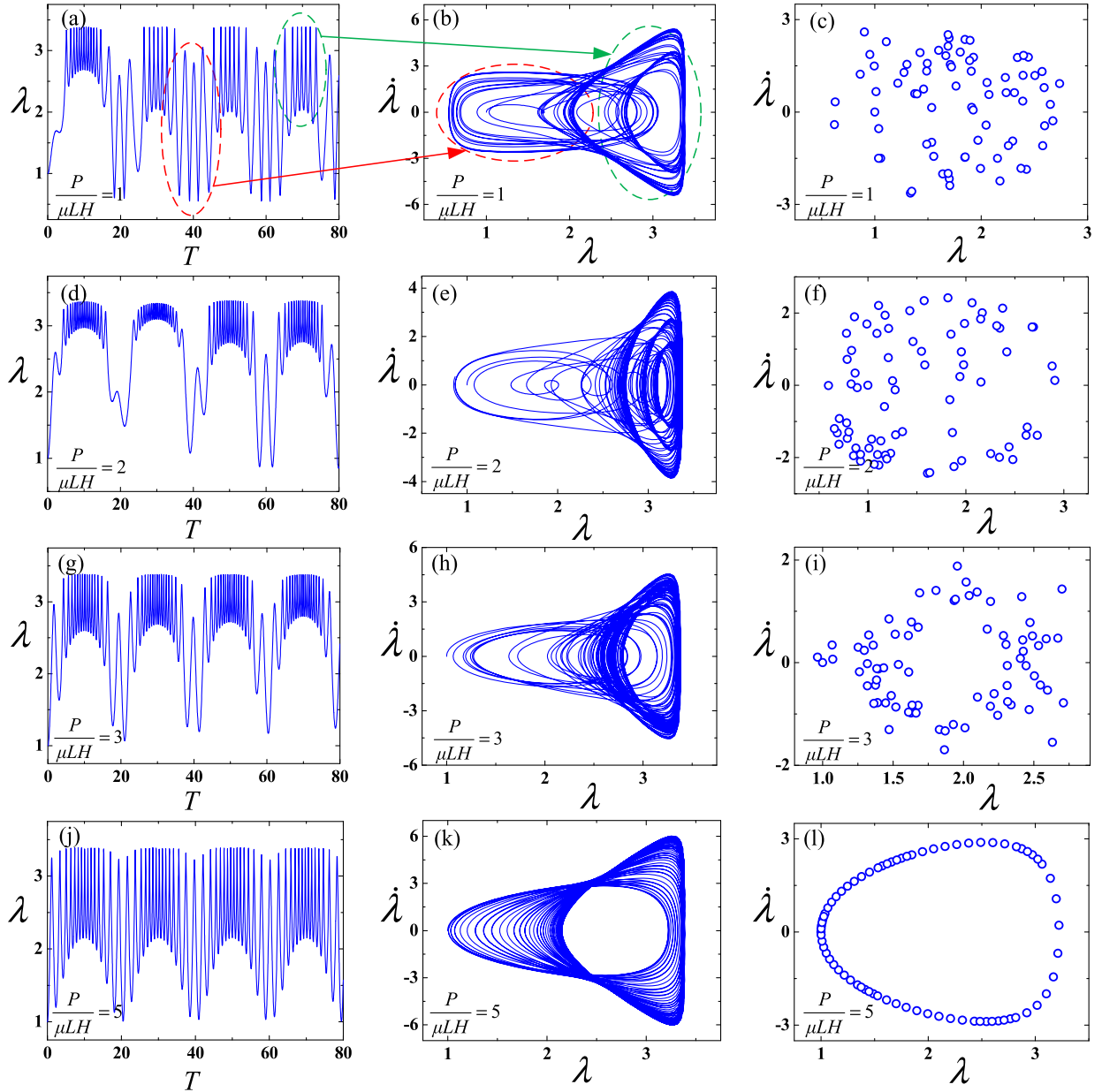


FIG. 9. Under the fixed dimensionless voltage amplitude of $\Phi_0 = 1$ and different mechanical tensile forces, the dynamic responses (a), (d), (g), (j); phase paths (b), (e), (h), (k); and Poincaré maps (c), (f), (i), (l) of DE with the limiting stretch of $J_{\text{lim}} = 20$. Four different dimensionless tensile forces are used in the calculation: $P/(\mu LH) = 1$ for (a), (b), (c); $P/(\mu LH) = 2$ for (d), (e), (f); $P/(\mu LH) = 3$ for (g), (h), (i); $P/(\mu LH) = 5$ for (j), (k), (l).

the 4th dimensionless period, as shown in Fig. 8(j). The Poincaré map in Fig. 8(l) also implies that the electro-mechanical failure occurs after the 3rd periods.

Combining Figs. 7 and 8, we conclude that the dynamic snap-through instability may emerge during vibration of DE. In contrast to the static snap-through behavior, occurring suddenly and being accomplished immediately, the dynamic snap-through behavior occurs more gently, and is accomplished in a short period. In addition, when applied voltage amplitude is small, the vibration is stable and without snap-through behavior. This is for the reason that a voltage

of small amplitude cannot attain the critical value that enables snap-through behavior to emerge. Furthermore, under the same excitation condition, a DE with a larger value of J_{lim} is more susceptible to snap-through instabilities and electro-mechanical failures.

C. Control dynamic snap-through instability by tuning tensile force

In the previous subsection, the dynamic snap-through behavior of DE under sinusoidal voltage is analyzed

without mechanical tensile forces applied. As is well known, in statics, mechanical prestretch and tensile load can eliminate the snap-through instability [14,15,19]. However, as actuators, the DEs are always connected to the external environment and undergo mechanical forces. In this case, the DEs can do work to external environment and avoid the occurrence of wrinkling and buckling when the prestretch is adopted. Therefore, in this subsection, we explore the property of dynamic snap-through instability by incorporating mechanical tensile forces. The DE with the limiting stretch of $J_{\text{lim}} = 20$ is utilized in this calculation case. The dimensionless amplitude of sinusoidal voltage is set as $\Phi_0 = 1$.

Figure 9 reveals the dynamic responses, phase paths, and Poincaré maps of DE under four groups of tensile forces. When the dimensionless tensile force is small, such as $P/(\mu LH) = 1$, the stretch vibrates in two regions in the time domain, as presented in Fig. 9(a). The two regions in time domain correspond to the two main orbits in the phase path in Fig. 9(b). The Poincaré map [Fig. 9(c)] under $P/(\mu LH) = 1$ is disordered and does not form a closed loop, indicative of an aperiodic vibration. With the increase of tensile force, e.g., $P/(\mu LH) = 2$, the snap-through behavior emerges gradually, and the vibration centers on the large value of stretch, as illustrated in Fig. 9(d). The phase path [Fig. 9(e)] and Poincaré map [Fig. 9(f)] under this condition suggest that the DE undergoes an aperiodic vibration. If the mechanical force is enlarged to $P/(\mu LH) = 3$, the snap-through behavior weakens and the two regions in time domain seem to appear, as plotted in Fig. 9(g). According to the phase path [Fig. 9(h)] and Poincaré map [Fig. 9(i)], the DE under $P/(\mu LH) = 3$ also experiences an aperiodic vibration. When the mechanical force increases to $P/(\mu LH) = 5$, the snap-through behavior disappears and the vibration becomes relatively stable, as shown in Fig. 9(j). The phase path [Fig. 9(k)] of DE under $P/(\mu LH) = 5$ is ordered, and the Poincaré map [Fig. 9(l)] forms a closed loop, demonstrating a quasiperiodic vibration.

Overall, tuning the tensile force can control the dynamic snap-through instability of DE. With the increase of tensile force, the dynamic snap-through behavior initially does not emerge during vibration, then accompanies the vibration, and disappears eventually. The stability of vibration also evolves from aperiodic to quasiperiodic. Hence, in practical application, the dynamic snap-through instability can be avoided by tuning the mechanical tensile force based on the selected workhorse DE material.

V. CONCLUSIONS

In this article, we develop a dynamics model to investigate the dynamic snap-through instability of DEs with different limiting stretches. Static snap-through instability, dynamic snap-through instability under triangle and sinusoidal voltages, and the method to

control the dynamic snap-through instability are studied, respectively. The main conclusions can be summarized as follows. In statics, a critical value of the limiting stretch exists, which determines the occurrence of snap-through instability. When the limiting stretch of DE material is below the critical value, the snap-through behavior is suppressed; while the limiting stretch of DE material exceeds the critical value, the snap-through behavior appears. When the DE is under a triangle voltage or a sinusoidal voltage, the snap-through behavior may emerge during the response in time domain, which is also determined by the value of the limiting stretch of DE material. A DE with a large value of limiting stretch is susceptible to dynamic snap-through instability. By tuning the mechanical tensile force, the occurrence of dynamic snap-through instability can be controlled. With the increase of tensile force, the dynamic snap-through behavior initially does not emerge during vibration, then accompanies the vibration, and disappears eventually. That is, the dynamic snap-through instability can be eliminated by tuning the external tensile force. The research results can be utilized to optimize the vibration of the practical DE oscillator and obtain a stable response without dynamic snap-through instability. However, viscoelasticity, an inherent property of macromolecular polymers, strongly affects the dynamic actuation performance of DEs. The dynamic snap-through behavior may be also altered by this inherent nature of DEs, which should be explored in future work.

ACKNOWLEDGMENTS

This research was supported by the China Postdoctoral Innovative Talents Supporting Program (Grant No. BX201600126), the China Postdoctoral Science Foundation (Grant No. 2016M600783), and the National Natural Science Foundation of China (Grants No. 51290294 and No. 11321062).

-
- [1] R. Pelrine, R. Kornbluh, Q. Pei, and J. Joseph, High-speed electrically actuated elastomers with strain greater than 100%, *Science* **287**, 836 (2000).
 - [2] F. Carpi, S. Bauer, and D. De Rossi, Stretching dielectric elastomer performance, *Science* **330**, 1759 (2010).
 - [3] P. Brochu and Q. Pei, Advances in dielectric elastomers for actuators and artificial muscles, *Macromol. Rapid Commun.* **31**, 10 (2010).
 - [4] X. Zhao and Z. Suo, Theory of Dielectric Elastomers Capable of Giant Deformation of Actuation, *Phys. Rev. Lett.* **104**, 178302 (2010).
 - [5] F. Carpi, I. Anderson, S. Bauer, G. Frediani, G. Gallone, M. Gei, C. Graaf, C. Jean-Mistral, W. Kaal, G. Kofod, M. Kolloosche, R. Kornbluh, B. Lassen, M. Matysek, S. Michel, S. Nowak, B. O'Brien, Q. Pei, R. Pelrine, B. Rechenbach,

- S. Rosset, and H. Shea, Standards for dielectric elastomer transducers, *Smart Mater. Struct.* **24**, 105025 (2015).
- [6] Q. Pei, M. Rosenthal, S. Stanford, H. Prahlaad, and R. Pelrine, Multiple-degrees-of-freedom electroelastomer roll actuators, *Smart Mater. Struct.* **13**, N86 (2004).
- [7] J. Zhang, H. Chen, L. Tang, B. Li, J. Sheng, and L. Liu, Modelling of spring roll actuators based on viscoelastic dielectric elastomers, *Appl. Phys. A* **119**, 825 (2015).
- [8] F. Carpi, G. Frediani, S. Turco, and D. De Rossi, Bio-inspired tunable lens with muscle-like electroactive elastomers, *Adv. Funct. Mater.* **21**, 4152 (2011).
- [9] S. Shian, R. M. Diebold, and D. R. Clarke, Tunable lenses using transparent dielectric elastomer actuators, *Opt. Express* **21**, 8669 (2013).
- [10] C. Keplinger, J.-Y. Sun, C. C. Foo, P. Rothemund, G. M. Whitesides, and Z. Suo, Stretchable, transparent, ionic conductors, *Science* **341**, 984 (2013).
- [11] K. Hochradel, S. J. Rupitsch, A. Sutor, R. Lerch, D. K. Vu, and P. Steinmann, Dynamic performance of dielectric elastomers utilized as acoustic actuators, *Appl. Phys. A* **107**, 531 (2012).
- [12] J. Zhou, L. Jiang, and R. E. Khayat, Investigation on the performance of a viscoelastic dielectric elastomer membrane generator, *Soft Matter* **11**, 2983 (2015).
- [13] C. C. Foo, S. J. A. Koh, C. Keplinger, R. Kaltseis, S. Bauer, and Z. Suo, Performance of dissipative dielectric elastomer generators, *J. Appl. Phys.* **111**, 094107 (2012).
- [14] C. Keplinger, T. Li, R. Baumgartner, Z. Suo, and S. Bauer, Harnessing snap-through instability in soft dielectrics to achieve giant voltage-triggered deformation, *Soft Matter* **8**, 285 (2012).
- [15] B. Li, H. Chen, J. Qiang, S. Hu, Z. Zhu, and Y. Wang, Effect of mechanical pre-stretch on the stabilization of dielectric elastomer actuation, *J. Phys. D* **44**, 155301 (2011).
- [16] Q. Wang and X. Zhao, Creasing-wrinkling transition in elastomer films under electric fields, *Phys. Rev. E* **88**, 042403 (2013).
- [17] K. Bertoldi and M. Gei, Instabilities in multilayered soft dielectrics, *J. Mech. Phys. Solids* **59**, 18 (2011).
- [18] X. Zhao, W. Hong, and Z. Suo, Electromechanical hysteresis and coexistent states in dielectric elastomers, *Phys. Rev. B* **76**, 134113 (2007).
- [19] T. Lu, J. Huang, C. Jordi, G. Kovacs, R. Huang, D. R. Clarke, and Z. Suo, Dielectric elastomer actuators under equal-biaxial forces, uniaxial forces, and uniaxial constraint of stiff fibers, *Soft Matter* **8**, 6167 (2012).
- [20] M. Kollosche, J. Zhu, Z. Suo, and G. Kofod, Complex interplay of nonlinear processes in dielectric elastomers, *Phys. Rev. E* **85**, 051801 (2012).
- [21] C. Keplinger, M. Kaltenbrunner, N. Arnold, and S. Bauer, Röntgen's electrode-free elastomer actuators without electromechanical pull-in instability, *Proc. Natl. Acad. Sci. U.S.A.* **107**, 4505 (2010).
- [22] B. Li, J. Zhou, and H. Chen, Electromechanical stability in charge-controlled dielectric elastomer actuation, *Appl. Phys. Lett.* **99**, 244101 (2011).
- [23] P. Dubois, S. Rosset, M. Niklaus, M. Dadras, and H. Shea, Voltage control of the resonance frequency of dielectric electroactive polymer (DEAP) membranes, *J. Microelectromech. Syst.* **17**, 1072 (2008).
- [24] J. Fox and N. Goulbourne, On the dynamic electromechanical loading of dielectric elastomer membranes, *J. Mech. Phys. Solids* **56**, 2669 (2008).
- [25] F. Chen, J. Zhu, and M. Y. Wang, Dynamic electromechanical instability of a dielectric elastomer balloon, *Europhys. Lett.* **112**, 47003 (2015).
- [26] J. Zhang, Y. Wang, D. McCoul, Q. Pei, and H. Chen, Viscoelastic creep elimination in dielectric elastomer actuation by preprogrammed voltage, *Appl. Phys. Lett.* **105**, 212904 (2014).
- [27] O. A. Araromi, S. Rosset, and H. R. Shea, High-Resolution, Large-Area Fabrication of Compliant Electrodes via Laser Ablation for Robust, Stretchable Dielectric Elastomer Actuators and Sensors, *ACS Appl. Mater. Interfaces* **7**, 18046 (2015).
- [28] D. Gatti, H. Haus, M. Matysek, B. Frohnapfel, C. Tropea, and H. F. Schlaak, The dielectric breakdown limit of silicone dielectric elastomer actuators, *Appl. Phys. Lett.* **104**, 052905 (2014).
- [29] J. G. Meier, J. W. Mani, and M. Klüppel, Analysis of carbon black networking in elastomers by dielectric spectroscopy, *Phys. Rev. B* **75**, 054202 (2007).
- [30] B. Li, J. Zhang, H. Chen, and D. Li, Voltage-induced pinnacle response in the dynamics of dielectric elastomers, *Phys. Rev. E* **93**, 052506 (2016).
- [31] Z. Suo, Theory of dielectric elastomers, *Acta Mech. Solida Sin.* **23**, 549 (2010).
- [32] J. Zhang, H. Chen, B. Li, D. McCoul, and Q. Pei, Coupled nonlinear oscillation and stability evolution of viscoelastic dielectric elastomers, *Soft Matter* **11**, 7483 (2015).
- [33] J. Zhou, L. Jiang, and R. E. Khayat, Dynamic analysis of a tunable viscoelastic dielectric elastomer oscillator under external excitation, *Smart Mater. Struct.* **25**, 025005 (2016).
- [34] T. Li, S. Qu, and W. Yang, Electromechanical and dynamic analyses of tunable dielectric elastomer resonator, *Int. J. Solids Struct.* **49**, 3754 (2012).
- [35] A. N. Gent, A new constitutive relation for rubber, *Rubber Chem. Technol.* **69**, 59 (1996).
- [36] T. Li, C. Keplinger, R. Baumgartner, S. Bauer, W. Yang, and Z. Suo, Giant voltage-induced deformation in dielectric elastomers near the verge of snap-through instability, *J. Mech. Phys. Solids* **61**, 611 (2013).
- [37] J. Zhang, B. Li, H. Chen, and Q. Pei, Dissipative performance of dielectric elastomers under various voltage waveforms, *Soft Matter* **12**, 2348 (2016).